Journal of Hepatocellular Carcinoma

Dovepress
Taylor & Francis Group

Open Access Full Text Article

ORIGINAL RESEARCH

Electroacupuncture and Moxibustion Regulate Aerobic Glycolysis and Alleviate Tumor Progression in Mice with Hepatocellular Carcinoma

Rui Zhong[1,*], Huangan Wu[1,2], Lu Zhu[1,2,*], Xiaowen Zhang[1,*], Yanxia Chen[1], Qin Qi[1,2], Guona Li[1], Zhaoqin Wang[1,2], Yan Huang[1,2], Zhihui Deng[1], Yuzhen Shi[1], Jing Li[1], Luyi Wu[1,2]

[1]Yueyang Hospital of Integrated Traditional Chinese and Western Medicine, Shanghai University of Traditional Chinese Medicine, Shanghai, People's Republic of China; [2]Shanghai Research Institute of Acupuncture and Meridian, Shanghai University of Traditional Chinese Medicine, Shanghai, People's Republic of China

*These authors contributed equally to this work

Correspondence: Luyi Wu; Jing Li, Yueyang Hospital of Integrated Traditional Chinese and Western Medicine, Shanghai University of Traditional Chinese Medicine, 110 Ganhe Road, Shanghai, 200437, People's Republic of China, Tel +8613917680799; +8618930568565, Email wuluyi@shutcm.edu.cn; LIJINGacu@126.com

Purpose: Aerobic glycolysis is crucial in the proliferation, metastasis, immunosuppression of hepatocellular carcinoma (HCC). We established mice model with HCC to explore whether electroacupuncture and moxibustion can alleviate HCC mice by inhibiting NSUN2-mediated aerobic glycolysis.

Methods: HCC mice model was established by intraperitoneal injection of diethylnitrosamine combined with carbon tetrachloride. In the moxibustion and electroacupuncture groups, the acupoints "Ganshu" and "Zusanli" (bilateral) were selected for intervention. Enzyme-linked immunosorbent assay quantified the serum levels. Immunohistochemistry/Western blotting, quantitative real-time PCR assessed protein and mRNA expressions of aerobic glycolysis. MRM-based targeted metabolomics quantified hepatic energy metabolism alterations.

Results: After HCC model completion on week 28, macroscopic examination revealed pronounced hepatomegaly with evident morphological distortion. The hepatic surface exhibited a coarse and irregular texture, accompanied by varying degrees of adhesions between adjacent liver lobes. Notably, large, well-defined tumors presenting in either whitish or dark-red appearances were observed scattered across the liver parenchyma. Following a total intervention period of 26 weeks, electroacupuncture and moxibustion significantly decreased the number of liver tumor, tumor load, mean tumor diameter and tumor volume compared to the model group ($P < 0.05$). Furthermore, the spleen and liver index were also significantly lowered ($P < 0.05$). A significant decrease was observed in the protein levels of serum AFP and AFP-L3 after treatment ($P < 0.05$). The protein and mRNA expression levels of NSUN2 and PKM2 were significantly downregulated ($P < 0.01$). Consistent with the inhibition of glycolytic flux, the protein expression of enzyme hexokinase 2 (HK2) was profoundly reduced ($P < 0.001$). Meanwhile, moxibustion decreased in the hepatic content of early glycolytic intermediates, glucose-6-phosphate (G6P) and fructose 6 phosphate (F6P) ($P < 0.01$), and electroacupuncture just decreased G6P ($P < 0.001$). Conversely, the level of phosphoenolpyruvate, a high-energy intermediate preceding the final step of glycolysis, was significantly elevated and increased ($P < 0.001$).

Conclusion: The study reveals that both electroacupuncture and moxibustion alleviate tumor proliferation in HCC mice by suppressing the NSUN2-PKM2 glycolytic axis, thereby highlighting this pathway as a novel metabolic target for non-pharmacological intervention; moreover, moxibustion uniquely exhibits the potential to induce a more extensive metabolic stress response. The observed reductions in tumor burden and key biomarkers corroborate the therapeutic potential of this approach. Collectively, these preclinical findings suggest that electroacupuncture and moxibustion, as non-pharmacological adjunctive therapies, hold translational potential for modulating tumor metabolism and slowing HCC progression, warranting further clinical investigation.

Keywords: hepatocellular carcinoma, electroacupuncture and moxibustion, NSUN2, PKM2, glycolysis

https://doi.org/10.2147/JHC.S577324
Received: 5 November 2025
Accepted: 27 January 2026
Published: 13 February 2026

Introduction

The global cancer statistics in 2020 shows that primary liver cancer (PLC) is sixth incidence rate in malignant tumors and currently the third leading cause of cancer-related death worldwide.[1] Hepatocellular Carcinoma (HCC) is the most common pathological type of PLC, accounting for 75–85% of all cases.[2] Liver cancer cells undergo extensive metabolic reprogramming, characterized by enhanced aerobic glycolysis, upregulated de novo lipogenesis, and accelerated amino acid metabolism—particularly glutaminolysis—which collectively provide the necessary energy, reducing equivalents, and biosynthetic precursors to fuel their rapid proliferation, invasion, and metastasis.[3–5] Aerobic glycolysis is pivotal in the proliferation, metastasis, immunosuppression and drug resistance of HCC, and the improvement of its process depends on the expression and activity of glycolytic enzymes and is closely related to the prognosis of HCC.[6,7] Hexokinase 2 (HK2), phosphofructokinase 1 (PFK1) and pyruvate kinase M2 (PKM2) are essential catalytic enzymes during the glycolysis.[6] An increasing evidence suggests that targeted glycolysis combined with existing therapeutic approaches may represent a novel strategy to enhance treatment responses and overcome drug resistance in patients with HCC.[8–10]

NOP2/Sun domain family member 2 (NSUN2) mediates epigenetic modification of m5C and is closely related to the occurrence and development of various cancers.[11–14] Previously, we identified that NSUN2-mediated m5C hypermethylation enhances aerobic metabolism in HCC by targeting PKM2 as a downstream effector in our investigation of HCC progression. We demonstrated that NSUN2-mediated m5C modification stabilizes PKM2 mRNA, thereby promoting glycolysis and driving HCC progression, offering a potential therapeutic target for patients with liver cancer.[15] Emerging evidence indicates that acupuncture modulates the DNA methylome in the colon of Crohn's disease model rats and regulates the landscape of epigenetic modifications, potentially mediated through its influence on the expression of DNA methyltransferases (DNMTs), ten-eleven translocation (TET) dioxygenases (responsible for DNA hydroxymethylation), and histone deacetylases (HDACs).[16–18] To date, the impact of acupuncture on epigenetic reprogramming in HCC remains unexplored. The study specifically investigates NSUN2—an RNA methyltransferase—and its role in orchestrating glycolytic flux, which may establish a mechanistic foundation for understanding acupuncture and moxibustion-mediated modulation of the epigenetic modification.

A substantial body of clinical and preclinical studies have explored the therapeutic or palliative effects of acupuncture in liver cancer. Clinical trials demonstrated that electroacupuncture can alleviate cancer pain in patients with advanced liver cancer, with its analgesic effect lasting longer than that achieved with transdermal drug patches.[19] Electroacupuncture at siguan acupoints combined with auricular acupressure demonstrates significant analgesic effects in patients with liver cancer pain and reduces the frequency of pain episodes.[20] In addition, experimental study have shown that acupuncture can inhibit the growth of tumor cells in mice bearing liver cancer.[21] Electroacupuncture may delay the tumor growth in HepG2 hepatocellular carcinoma-bearing nude mice by modulating miRNA-involved protein metabolic, cancer-related signaling, and MAPK signaling pathway.[22]

Electroacupuncture and moxibustion, while both rooted in traditional acupoint stimulation, represent two distinct physical modalities with potentially different primary mechanisms. Electroacupuncture delivers pulsed electrical currents, which are primarily transduced via somatosensory neural pathways to modulate systemic neuroendocrine and inflammatory responses.[19,20] Moxibustion applies localized heat and bioactive compounds from burning moxa wool, which may exert effects through activation of thermosensitive receptors and direct pharmacological modulation of local tissue.[23] Given that metabolic dysregulation in HCC is influenced by both neural signaling and the local inflammatory microenvironment, this study was designed to conduct a comparative investigation of these two interventions.

Among patients with advanced liver fibrosis and cirrhosis, nearly 90% ultimately develop hepatocellular carcinoma.[24] Therefore, our study utilized a mouse model of HCC induced by diethylnitrosamine (DEN) combined with carbon tetrachloride (CCl4) to simulate the inflammation to cancer transition in the liver. By focusing on NSUN2-mediated glycolysis, the research aims to investigate the effects and mechanisms of moxibustion and electroacupuncture in the prevention and treatment of HCC.

Materials and Methods

Animal Experiment and Reagents

Male C57BL/6J mice (3 weeks old) were obtained from the Shanghai Slack Experimental Animal Co., Ltd. (License No: SCXK (Shanghai) 2017–0005) and housed under specific pathogen-free conditions at 20 ± 2°C with a 12-hour light/dark cycle.

Introduction of HCC Models

HCC models were prepared by intraperitoneal injection of DEN and CCl4 according to previous study.[25] The mice received a single intraperitoneal injection of DEN (Macklin, China) at 4 weeks of age, with a dose of 20μL/g body weight (preparation: dissolve 26.3μL of the DEN stock solution in 20 mL of normal saline). Starting from 6 weeks of age, mice were given intraperitoneal injections of CCl4 once a week, with a dose of 5μL/g body weight (diluted according to a CCl4 (Wokai, China) and olive oil (Macklin, China)), and the injections continued for 25 weeks before ending (Figure 1). At the end of the experiment, liver and blood samples were collected, mouse was taken for pathological observation of the liver by hematoxylin and eosin (H&E) staining, and the next intervention was performed when the success of modeling was confirmed.

Blinding and Operator Standardization

For all animals, three different investigators were involved as follows: a first investigator exclusively maintained and executed the randomization schedule. A second investigator was responsible for the treatment procedure, whereas a third investigator performed the outcome assessment to ensure complete separation between randomization, experimental procedures and assessment. All acupuncturists will undergo comprehensive standardized training, which includes unified didactic instruction, supervised practical sessions, and interactive webinars, to ensure consistent application of the treatment protocol across all operators.

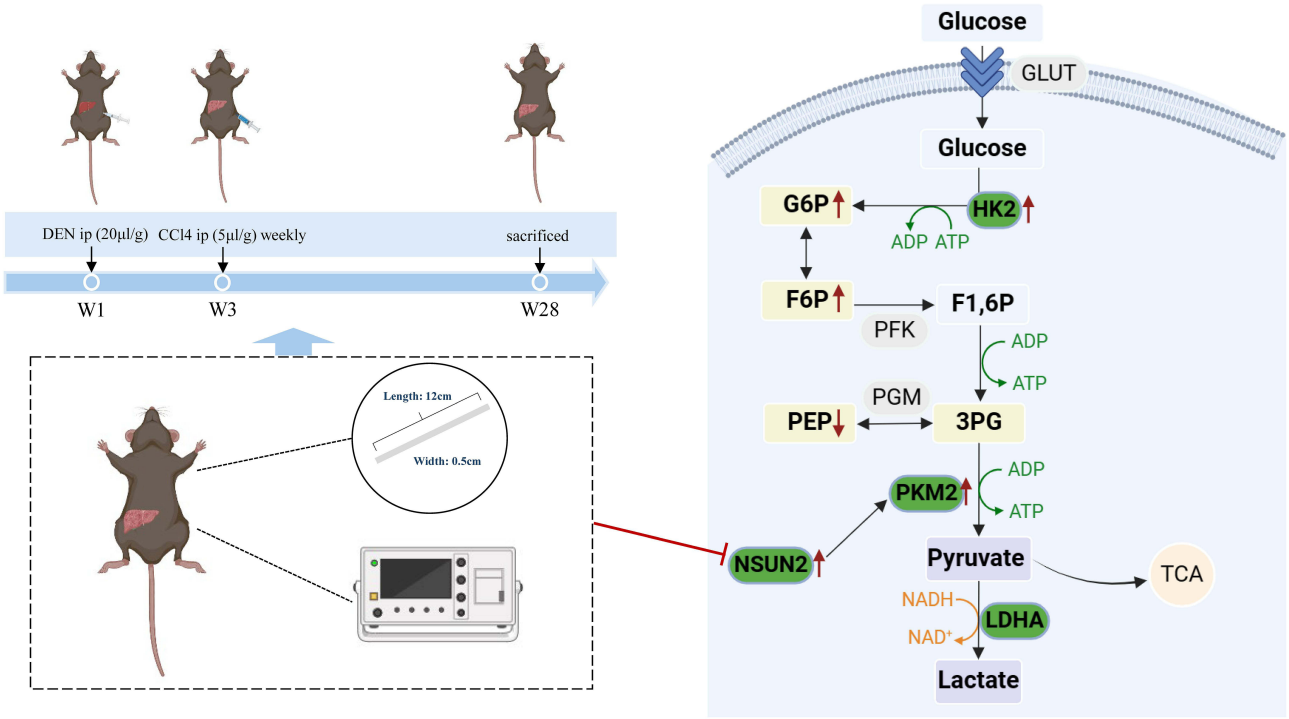

Figure 1 Schematic diagram illustrating the experimental design to elucidate the therapeutic mechanism of electroacupuncture and moxibustion. Electroacupuncture and moxibustion suppress tumor progression of HCC mice by downregulating NSUN2 expression and subsequently inhibiting PKM2-mediated glycolysis. The red arrows represent the molecular target. Figure created with BioRender.

https://doi.org/10.2147/JHC.S577324

Grouping and Intervention

Mice were randomly divided into four groups: normal group (NG), model group (MG), moxibustion group (MOX) and electroacupuncture group (EA). As a normal control, mice in NG were not intervened, and other remaining mice were induced to be HCC models. The mice in NG and MG did not receive active treatment but were subjected to the same restraint procedure as the treatment groups. In MOX group and EA group, moxibustion and electroacupuncture intervention were performed during modeling to verify the inhibition of them. Electroacupuncture was performed at bilateral BL18 (Ganshu) and ST36 (Zusanli) acupoints using sterile disposable needles (diameter: 0.16 mm, length: 13 mm; Suzhou Huatuo Medical Instrument Co., Ltd., China), which were inserted to a depth of 3–4 mm. Acupoint stimulation was administered alternately on the left and right sides across sessions to minimize localized tissue irritation. In EA group, the needles were connected to an EA apparatus (HANS-200A, Nanjing Jisheng Medical Technology, China) and stimulated with a continuous waveform at a frequency of 2 Hz and an intensity of 1 mA. The current intensity was adjusted to induce slight local muscle twitching without causing evident distress to the animals. Stimulation was applied for 10 minutes per session, three times per week, over a total period of 26 weeks. Throughout the study, a specialized rodent restraint device was used for all handling procedures to ensure consistency and minimize stress. Specific moxa sticks (Nanyang hanyiairong, Henan, China) were performed as same as that of EA group (Figure 1).

Sample Collection and Processing

After the intervention, 1% pentobarbital sodium (40–50mg/kg) was injected into abdominal cavity for anesthesia. Once the mice were anesthetized, glass spotting capillary needles were inserted into bilateral orbital veins of mice, and venous blood was collected in centrifuge tubes. One hour after equilibration, blood was placed in a centrifuge with 3000 rpm for 10 minutes at 4°C to retain the supernatant. After mouse euthanasia through cervical dislocation, the abdomen was quickly opened, the spleen and liver were taken and weighed. The shape, color, texture and number of liver tumors were observed. The tumor size was measured and recorded and a part of them were stored in a refrigerator at −80°C, and the rest were fixed in 4% paraformaldehyde.

Enzyme-Linked Immunosorbent Assay (ELISA)

Blood samples were collected and centrifuged to retain the supernatant. The AFP and AFP-L3 level were measured using AFP and AFP-L3 ELISA kits (Enzyme linked Biotechnology, Shanghai, China). The absorbance at 450 nm was measured by a microplate reader (BioTek, USA).

Tumor Proliferation, Spleen and Liver Index

Tumor volume (mm^3) = 0.5 × length × width.[2,26] The tumor load was the sum of the diameters of all tumors in mice liver. The tumor number was the number of tumors observed in the liver of per mouse. The average tumor diameter/volume was the mean value of all tumor diameters/volumes observed in the liver of per mouse. Spleen index = Spleen wet weight/body mass × 100%. Liver index = Liver wet weight/body mass × 100%.

H&E Staining

Liver tissues were embedded in 4% paraformaldehyde for 24 h and then embedded in paraffin, sectioned at a thickness of 4 μm. Slices were baked in an oven at 60°C for 1 h; And put the slices into xylene and gradient alcohol (100%, 90%, 80%, 70%, each for 5 min) in turn for dewaxing. After the slices were stained with hematoxylin and eosin staining; put into alcohol and xylene for dehydration and transparency. Finally, the neutral gum was sealed, dried, observed and photographed under a microscope (Olympus Corporation, Japan).

Immunohistochemistry (IHC)

Immunohistochemistry was performed to characterize the expression of NSUN2 and PKM2. Slides were deparaffinized with xylene and gradient alcohol for dewaxing, and citrate was used for antigen retrieval in a microwave oven. Endogenous peroxidase activity was blocked using 3% H_2O_2 for 30 min at room temperature in the dark, then 5% BSA was blocked for 1 h at room temperature. Slides were performed with primary rabbit anti-NSUN2 (1:500, Abcam,

UK) and anti-PKM2 antibodies (1:500, CST, USA) overnight at 4°C. The next day, HRP conjugate anti-rabbit secondary antibody (Beyotime, Shanghai, China) was added dropwise and color development expressed by DAB kit (Boster, Wuhan, China) for 5 min. Three different fields of view under the same magnification were randomly selected to take photos, and Image J software was used for image acquisition and analysis.

RNA Isolation and Quantitative Real-Time Polymerase Chain Reaction (qRT-PCR)

qRT-PCR was employed to evaluate the expression levels of NSUN2, NSUN6, PKM2. Total RNA extraction was carried out with SteadyPure Universal RNA Extraction Kit (Aikeraite, Hunan, China). cDNA was synthesized by Evo M-MLV RT Premix for qPCR (Aikeraite, Hunan, China). And then qPCR was performed with SYBR Green Premix Pro Taq HS qPCR Kit (Aikeraite, Hunan, China). The relative amounts of transcripts were calculated by the $2^{-\Delta\Delta Ct}$. The primer sequences were listed in Table 1.

Western Blotting

The protein expression levels of NSUN2, HK2 and LDHA were detected by Western blotting. Livers tissues were pulverized in liquid nitrogen and lysed in a Column Tissue & Cell Protein Extraction Kit (EpiZyme, Shanghai, China) containing protease inhibitor and RIPA buffer. Protein concentrations were quantified, and 40 μg of each sample was separated by SDS-PAGE (10%) and transferred to a PVDF membrane (Millipore, Boston, MA, USA). Membranes were blocked with 5% skim milk (EpiZyme, Shanghai, China) for 1 h at room temperature and gently shaken overnight with anti-NSUN2 (1:1000, Abcam, UK), anti-HK2 (1:1000, SAB, USA), anti-LDHA (1:1000, SAB, USA) and anti-β-actin (1:2000, Beyotime, China), respectively, at 4°C. The membrane was incubated with a secondary antibody (Beyotime, Shanghai, China) for 1 h. Finally, the signal was detected by Omni-ECL™ Femto Light Chemiluminescence Kit (EpiZyme, Shanghai, China) and visualized with the Image J software.

Targeted Metabolomics

Liver tissues were vortexed for 60 seconds, and then add methanol and acetonitrile solution and vortex for 60 seconds; centrifuge at low temperature for 30 minutes, repeat twice; let stand for 1 h at −20°C; centrifuge at 14000rcf centrifugal force, centrifuge at 4°C for 20 minutes, and take the supernatant and store at-80°C. Samples were separated using an ultra-performance liquid chromatography system (Agilent, USA). Place 2 μL of the sample to be tested in the injector, the column temperature was 45°C, and the flow rate was 300 μL/min; the liquid phase gradient was as follows: 0–18 minutes, solution B changed linearly from 90% to 40%; 18–18.1 minutes, solution B changed linearly from 40% to 90%; 18.1–23 minutes, solution B remained at 90%. Mass spectrometry analysis is performed in negative ion mode, MRM mode is used to detect the ion pairs to be tested, and ion pair information of all energy metabolites is retained. Multiquant software extracts chromatographic peak areas and retention times, and corrects retention times using standards for energy metabolizing substances (Sigma-Aldrich, USA) to identify metabolites.

Table 1 Primer Sequences

Genes	Primer Sequences (5′ to 3′)
NSUN2	Forward Primer: ACACTGAGAATCACTGGGTACA
	Reverse Primer: CCAGCTTAGTGGTTGTGGAACT
PKM2	Forward Primer: CGCCTGGACATTGACTCTG
	Reverse Primer: GAAATTCAGCCGAGCCACATT
NSUN6	Forward Primer: AAGACAACAGGGTGAAGTGATTG
	Reverse Primer: TCCATCAAATTCTTTGGCTCCTT
β-Actin	Forward Primer: GTGACGTTGACATCCGTAAAGA
	Reverse Primer: GCCGGACTCATCGTACTCC
GAPDH	Forward Primer: AGGTCGGTGTGAACGGATTTG
	Reverse Primer: TGTAGACCATGTAGTTGAGGTCA

https://doi.org/10.2147/JHC.S577324

Statistical Analysis

All data were conducted by SPSS 26.0 statistical software and showed with GraphPad Prism 10.0 Software. When the data is normally distributed, it is expressed as mean ± SD and was analyzed using one-way ANOVA followed by post hoc Tukey's multiple comparison test. For data that does not conform to normality, data was expressed as the median (*P*25, *P*75) and analyzed using Kruskal −Wallis. $P < 0.05$ was considered statistically significant.

Results

Moxibustion and Electroacupuncture Alleviate Liver Damage and Prevent Liver Tumor Development in HCC Mice

We observed and photographed mice liver tissue. The images showed that the liver surface of mice in NG was smooth, light red, soft in texture, irregular in shape. The liver of mice in MG showed rough and uneven surfaces, many granular round protuberances of different sizes, and local white or dark red tumors, with tumors spreading over blood vessels (Figure 2A). Compared with MG, the number of liver tumors, tumor load, the average diameter of tumors and the

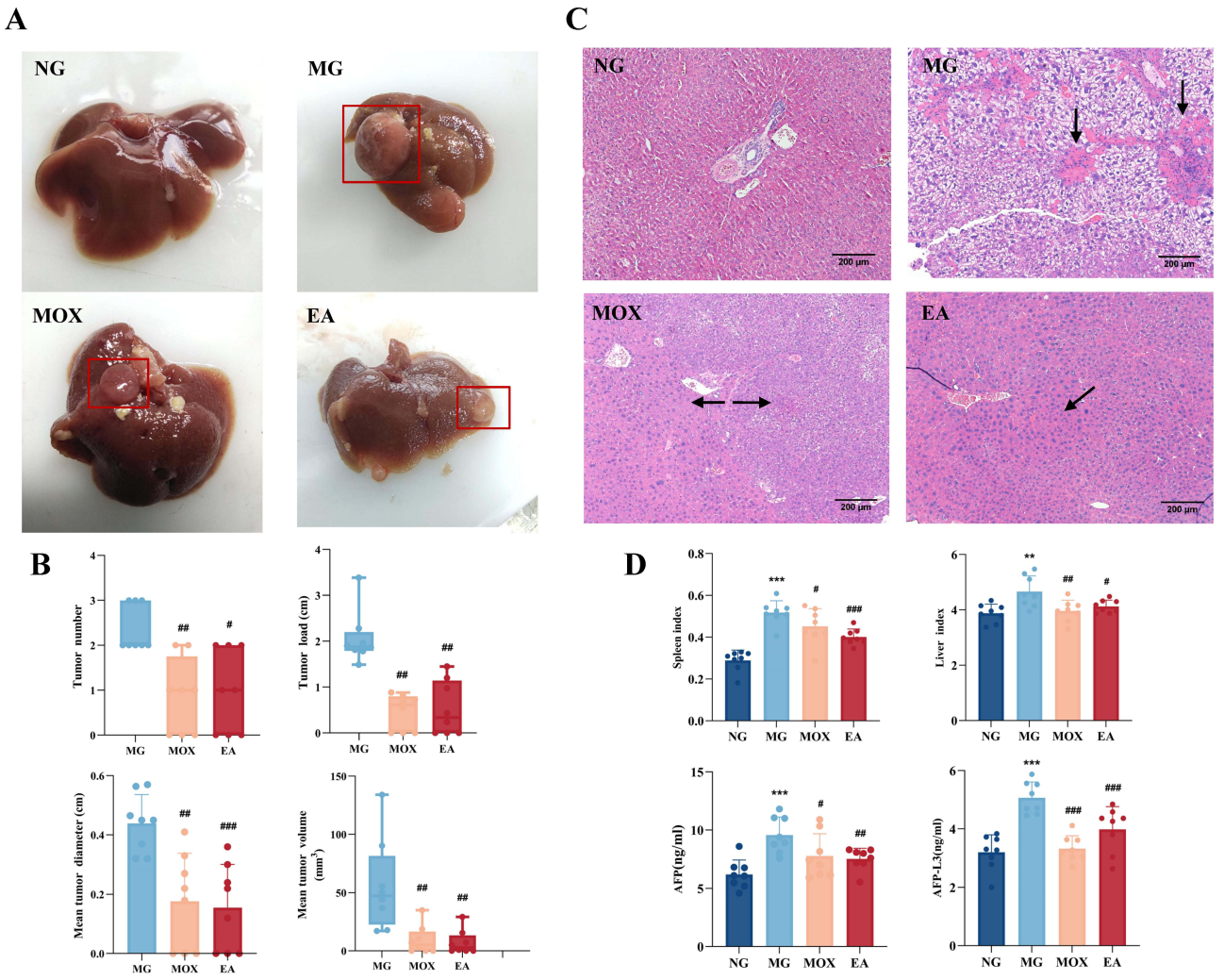

Figure 2 (**A**) Representative macroscopic images of tumors in the livers of mice. (**B**) Comparison of the number of liver tumor, tumor load, mean tumor diameter and tumor volume. (**C**) Morphological observation of H&E-stained liver sections (magnification: ×100). Arrows indicate tumor tissues or damaged sites. (**D**) Comparison of the spleen index, liver index, and the AFP and AFP-L3 expression levels in blood. (n = 8). The red marked boxes show the tumors and the black arrows point to the liver damage site. Compared with NG, $^{***}P < 0.001$, $^{**}P < 0.01$; compared with MG, $^{\#\#\#}P < 0.001$, $^{\#\#}P < 0.01$, $^{\#}P < 0.05$.
Abbreviations: NG, normal group; MG, model group; MOX, moxibustion group; EA, electroacupuncture group.

https://doi.org/10.2147/JHC.S577324

average volume of tumors were significantly smaller in MOX and EA group ($P < 0.05$), and with fewer blood vessels compared with MG mice (Figure 2B).

H&E staining showed the hepatic lobule structure in NG mice was intact, with hepatocytes arranged radially and nucleoli and nuclear membranes clearly defined. However, the structure of hepatic cords and sinusoids in MG was disrupted, central veins were displaced, and tumor boundaries were indistinct. Tumor tissues appeared irregular or in clusters, with some nuclei exhibiting enlarged, hyperchromatic, and irregular shapes, accompanied by severe hepatocyte vacuolization and extensive infiltration of inflammatory cells. The normal hepatic structure was preserved in MOX and EA, although some cytoplasm exhibited small vacuoles, and clusters of necrotic and regenerating hepatocytes were observed (Figure 2C).

The spleen index and liver index of mice in MG were significantly increased than those in NG (spleen index, $P < 0.001$; liver index, $P < 0.01$) and a decreased occurred (spleen index, $P < 0.001$, $P < 0.05$) after moxibustion, but there was no statistical difference in liver index (Figures 2D). Meanwhile, the serum AFP and AFP-L3 contents of mice in MG were significantly higher than those in NG (AFP, $P < 0.001$; AFP-L3, $P < 0.001$), but they were reduced after moxibustion and electroacupuncture (AFP, $P < 0.001$, $P < 0.05$; AFP-L3, $P < 0.001$, $P < 0.01$) (Figure 2D). The results suggest that moxibustion and electroacupuncture can reduce the spleen index in mice, inhibit the expression of AFP and AFP-L3 delaying tumor proliferation in HCC mice during the progression of HCC.

Moxibustion and Electroacupuncture Inhibit NSUN2 and Enzyme PKM2 in HCC Mice

To explore the influence of NSUN2 and PKM2 in HCC mice and whether moxibustion and electroacupuncture alleviate liver damage and prevent liver tumor procession through NSUN2 and PKM2, IHC were used to detect the expression of NSUN2 and PKM2 in each group. The protein expression of NSUN2 and PKM2 were significantly higher than that in NG (NSUN2, $P < 0.05$; PKM2, $P < 0.001$). In MOX and EA group, the expression of NSUN2 and PKM2 was reduced comparing to MG (NSUN2, $P < 0.05$; PKM2, $P < 0.001$, $P < 0.01$) (Figure 3A–C).

Then, we conducted the mRNA levels of NSUN2, PKM2 and NSUN6 by qRT-PCR. As shown in Figure 3D and E, the mRNA expression of NSUN2 and PKM2 was increased in MG (NSUN2, $P < 0.001$; PKM2, $P < 0.01$), but their expression was decreased in MOX and EA group (NSUN2, $P < 0.001$, $P < 0.01$; PKM2, $P < 0.05$). However, there was no statistical difference in the mRNA levels of NSUN6 (Figure 3F).

Moxibustion and Electroacupuncture Prevent the Progression of HCC in Mice by Inhibiting Glycolysis

Quality control standard display that metabolites have good chromatographic separation with sharp and symmetrical peak shapes, allowing mass spectrometry quantification (Figure 4A). All samples were mixed in equal amounts to prepare QC samples, and QC samples were used to evaluate the stability and repeatability of the data. The RSD of energy metabolism was less than 30%, indicating that the data was stable and reliable (Figure 4B). Heatmap showed differences in glycolysis-related metabolic products of liver among the NG and MG groups (Figure 4C), the MG and EA groups (Figure 4D), the MG and MOX groups (Figure 4E).

To verify the function of moxibustion and electroacupuncture on glycolysis of HCC, we analyzed glycolysis-related metabolic products in liver tissues. According to Figure 5A–I, compared with NG, the relative contents of G6P, F6P, guanosine 5′-monophosphate (GMP), and adenosine monophosphate (AM) in MG increased significantly ($P < 0.001$), and the relative contents of 3-phospho-D-glycerate (3PG) and PEP decreased (3PG, $P < 0.001$; PEP, $P < 0.01$). Compared with MG, the relative contents of G6P and AM decreased, but the content of PEP increased ($P < 0.05$) after moxibustion and electroacupuncture. While moxibustion can also additionally reduce the relative contents of F6P, GMP ($P < 0.05$).

Moxibustion and Electroacupuncture Prevent the Development of HCC in Mice by Inhibiting NSUN2-Mediated Glycolysis

We further extracted the main enzymes in glycolysis using Western blot analysis, including NSUN2, HK2 and lactate dehydrogenase A (LDHA). As the results showed, the protein expression of NSUN2 and HK2 was significantly increased

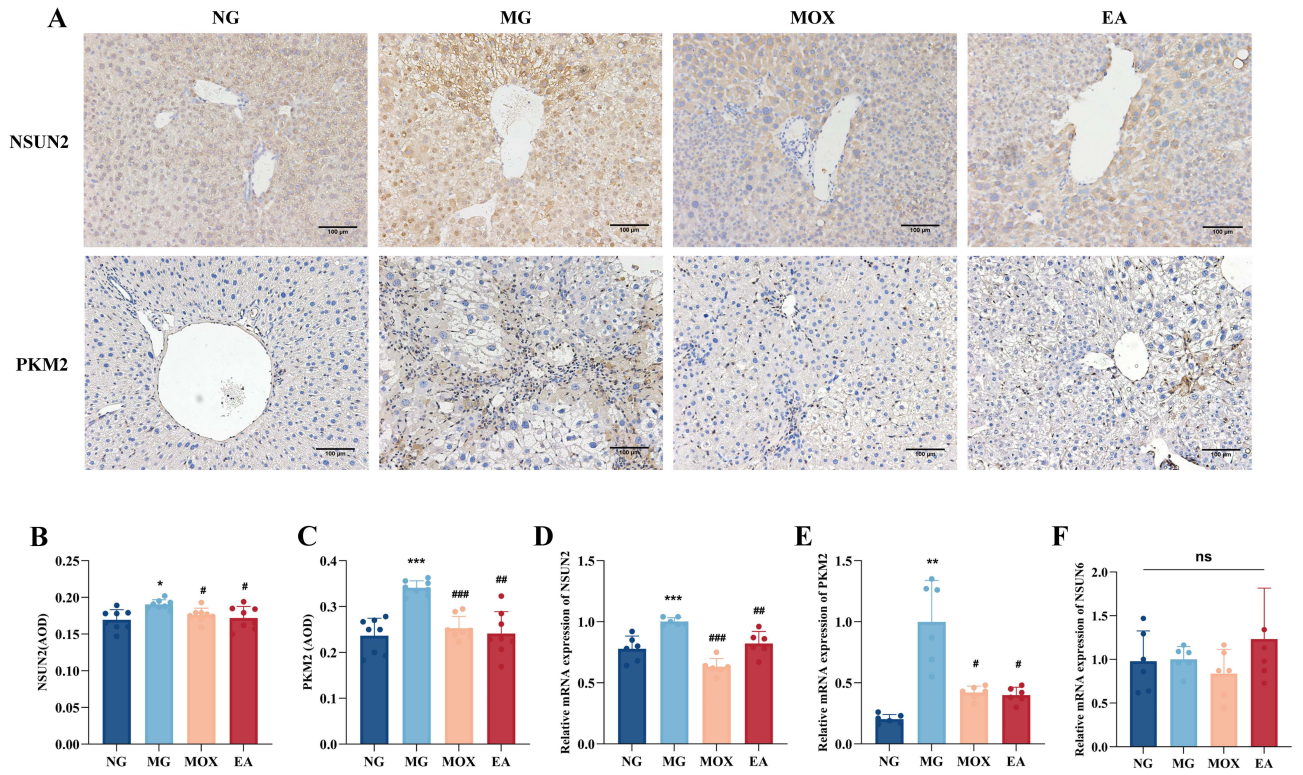

Figure 3 (**A**) IHC staining of NSUN2 and PKM2 in liver tissues (magnification: ×200). Comparison of NSUN2 (**B**) and PKM2 (**C**) expression levels measured by IHC. (n = 8). Relative NSUN2 (**D**), PKM2 (**E**) and NSUN6 (**F**) mRNA expression levels were determined by qRT-PCR in HCC mice. (n = 6). Compared with NG, ***$P < 0.001$, **$P < 0.01$, *$P < 0.05$; compared with MG, $^{\#\#\#}P < 0.001$, $^{\#\#}P < 0.01$, $^{\#}P < 0.05$; ns: no significant difference.

Abbreviations: NG, normal group; MG, model group; MOX, moxibustion group; EA, electroacupuncture group.

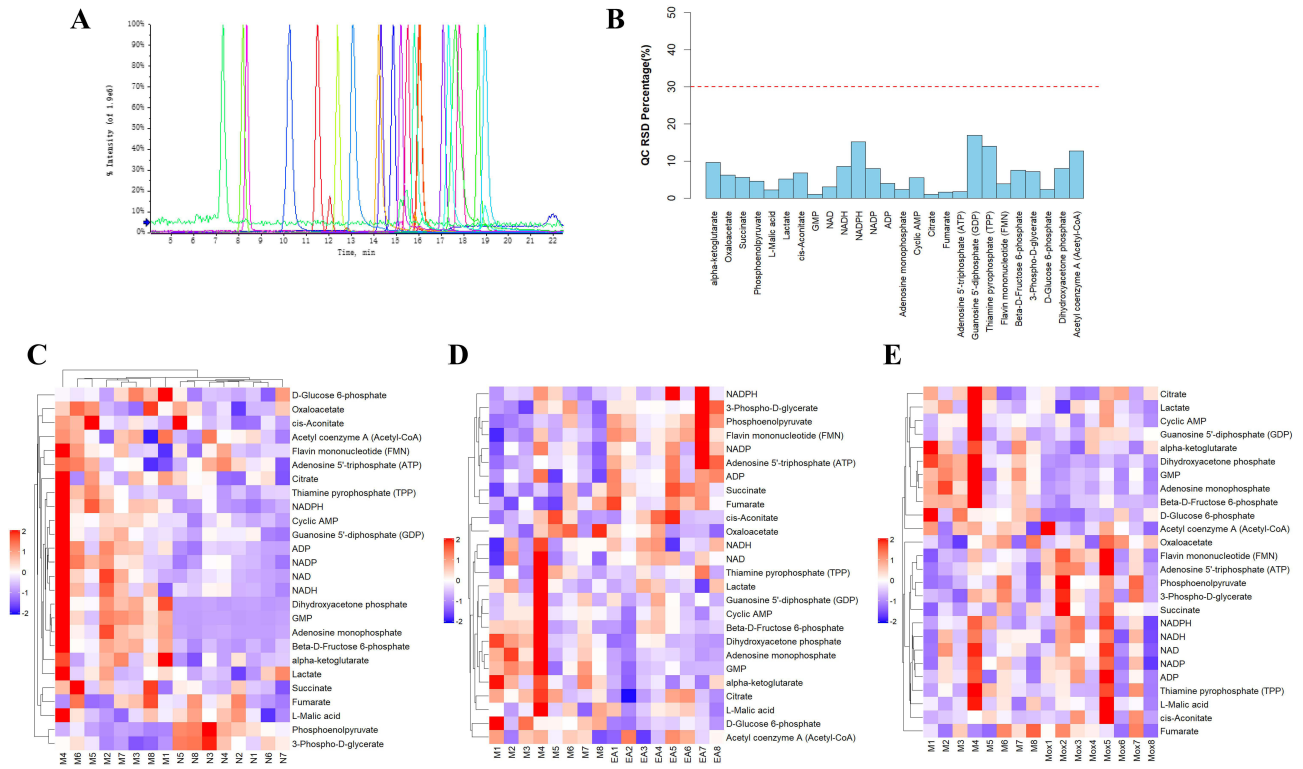

Figure 4 (**A**) XIC diagram of standard mixture; (**B**) RSD distribution plot; (**C**) Heatmap of differential metabolic products in the liver of the N and M groups; (**D**) Heatmap of differential metabolic products in the liver of the M and EA groups; (**E**) Heatmap of differential metabolic products in the liver of the M and MOX groups.

https://doi.org/10.2147/JHC.S577324

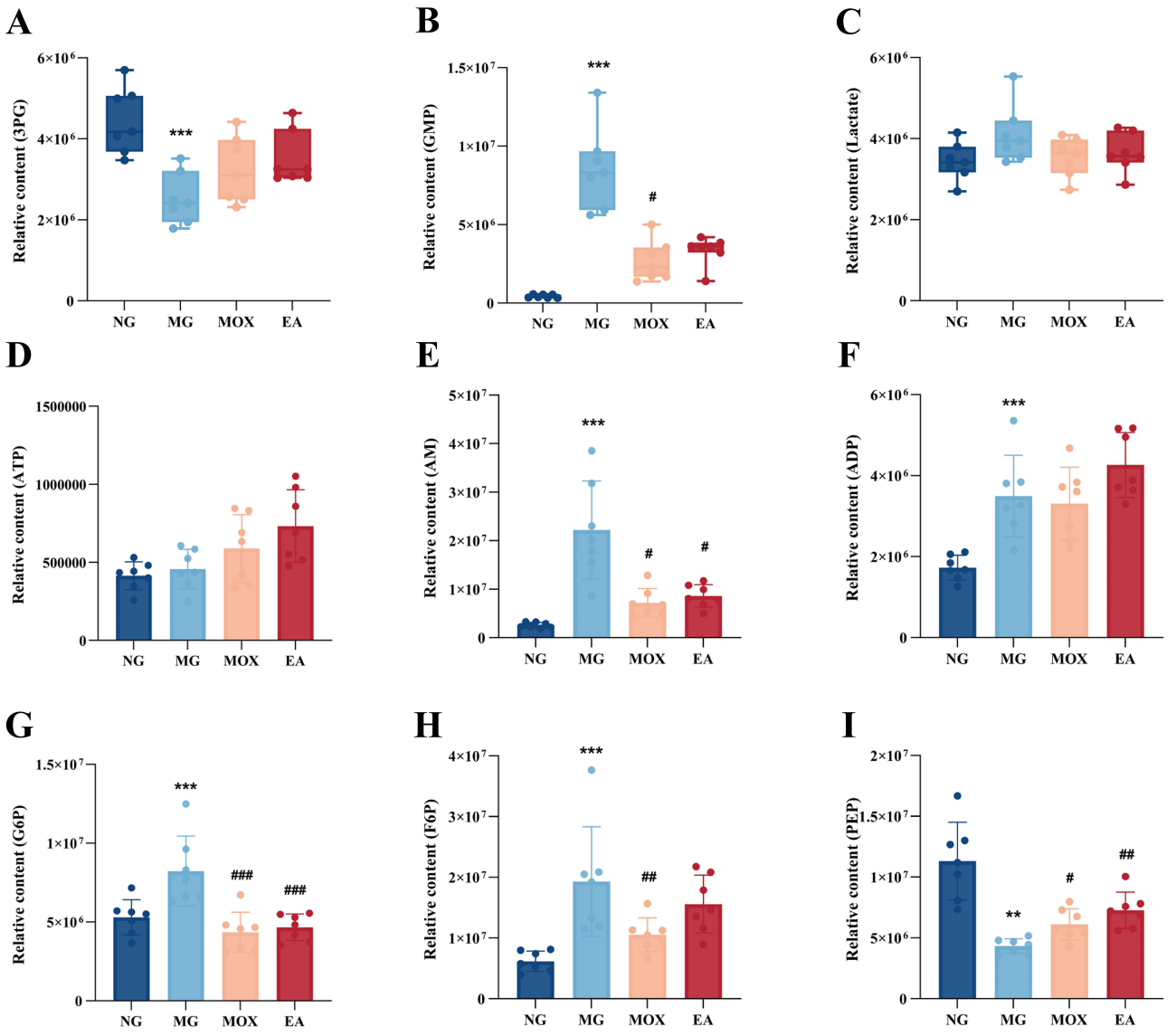

Figure 5 (**A**) Relative contents of 3PG; (**B**) Relative contents of GMP; (**C**) Relative contents of Lactate; (**D**) Relative contents of ATP; (**E**) Relative contents of AM; (**F**) Relative contents of ADP; (**G**) Relative contents of G6P; (**H**) Relative contents of F6P; (**I**) Relative contents of PEP. (n = 7). Compared with NG, $^{***}P < 0.001$, $^{**}P < 0.01$; compared with MG, $^{\#\#\#}P < 0.001$, $^{\#\#}P < 0.01$, $^{\#}P < 0.05$.

Abbreviations: NG, normal group; MG, model group; MOX, moxibustion group; EA, electroacupuncture group.

in MG ($P < 0.001$), but a decrease occurred after moxibustion and electroacupuncture (NSUN2, $P < 0.01$; HK2, $P < 0.001$) (Figure 6A–D). However, there was no statistical difference in the protein levels of LDHA (Figure 6E and F).

Discussion

Due to the lack of early diagnostic biomarkers with high specificity and sensitivity in clinical practice, combined with the inherently high metastatic potential of HCC, the overall survival rate of HCC patients remains extremely low. Therefore, identifying novel biomarkers and therapeutic targets is of great significance for improving the diagnosis and treatment of HCC. HCC is a classic example of inflammation-driven carcinogenesis. The progression of chronic hepatic inflammation leads to liver fibrosis and ultimately cirrhosis, under which conditions nearly 90% of cirrhotic patients eventually develop HCC.[24] In experimental research, the murine model induced by chemical hepatotoxins such as diethylnitrosamine (DEN) and carbon tetrachloride (CCl4), which recapitulates the inflammation to cancer transformation in the liver, remains

https://doi.org/10.2147/JHC.S577324

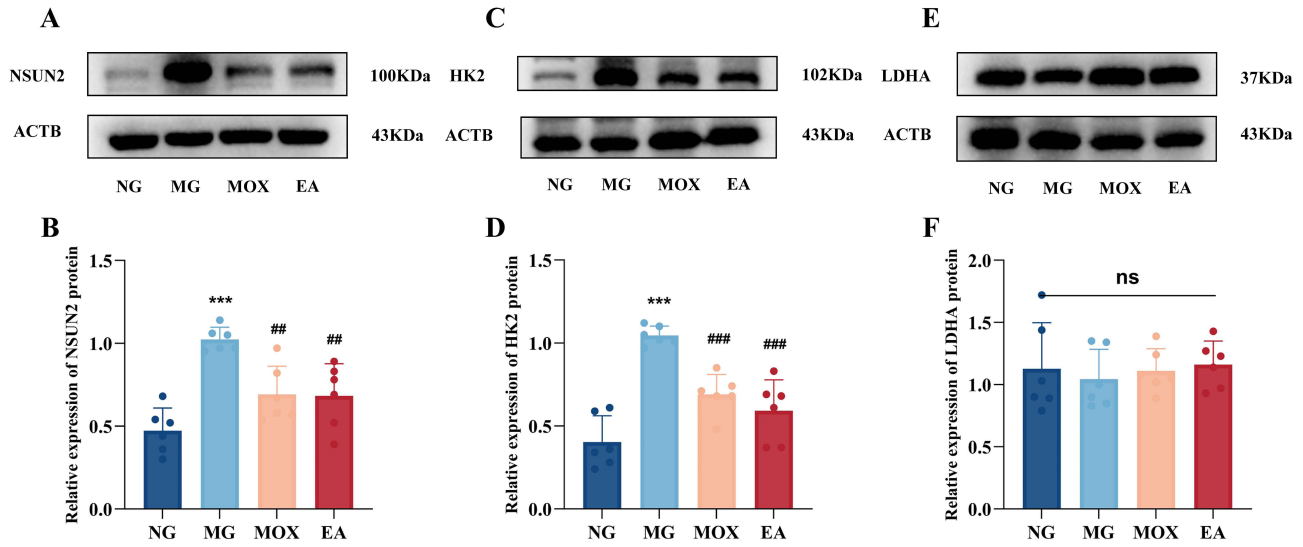

Figure 6 (**A**) Western blotting detection of NSUN2 protein expression in liver. (**B**) Comparison of the relative protein expression of NSUN2 in glycolysis; (**C**) Western blotting detection of HK2 protein expression in liver. (**D**) Comparison of the relative protein expression of HK2 in glycolysis; (**E**) Western blotting detection of LDHA protein expression in liver. (**F**) Comparison of the relative protein expression of LDHA in glycolysis. (n = 6). Compared with NG, $^{***}P < 0.001$; compared with MG, $^{\#\#\#}P < 0.001$, $^{\#\#}P < 0.01$; ns: no significant difference.

Abbreviations: NG, normal group; MG, model group; MOX, moxibustion group; EA, electroacupuncture group.

a classic and widely utilized model system for HCC studies.[27] This model provides a valuable platform for in-depth investigation into the pathogenesis of HCC and for the preclinical evaluation of novel therapeutic strategies.

The treatment landscape for HCC is diverse and stage-dependent. For very early-stage HCC, local ablation therapies such as radiofrequency ablation are considered first-line options.[28] Surgical interventions, including liver resection and transplantation, remain the optimal curative approaches that significantly prolong overall survival4. In intermediate to advanced stages, combination therapies are commonly employed, such as transarterial chemoembolization (TACE) combined with radiofrequency ablation or TACE followed by surgical resection.[29] In recent years, acupuncture and moxibustion have often been combined with other therapies for the treatment of HCC, demonstrating advantages in inhibiting tumor growth, reducing adverse effects, alleviating clinical symptoms, improving quality of life, and prolonging survival.[30–33] Notably, clinical report suggested that combining moxibustion with immunotherapy and targeted drugs in the management of primary HCC may lead to sustained tumor reduction, an absence of drug-related adverse effects, and extended patient survival, indicating potential synergistic efficacy.[31] Furthermore, when integrated with conventional therapies, acupuncture has been shown to improve survival rates, suppress tumor progression, and enhance performance status in patients with intermediate to advanced HCC.[32] Our previous study have found that percutaneous acupuncture point electrical stimulation significantly enhances analgesic effects and, to some extent, reduces gastrointestinal side effects caused by medications, alleviating severe pain in liver cancer patients.[30] Lai et al found that electroacupuncture significantly reduced tumor volume and increased the levels of $CD4^+$T cells and the $CD4^+/CD8^+$ ratio in peripheral blood.[34] Wang et al demonstrated that electroacupuncture delayed the growth trend of HepG2 cells, suggesting that the tumor-controlling effect may be associated with miR-409-5p-mediated targeted inhibition of the TGF-β1 signaling pathway.[35] Recent studies have shown that electroacupuncture at Zusanli (ST36) can promote hepatocyte proliferation and liver regeneration by activating cholinergic neurons in the dorsal motor nucleus of the vagus nerve, which induces acetylcholine release from hepatic vagal terminals; this acetylcholine then acts in synergy with IL-6 released from hepatic macrophages via cholinergic receptors.[36] As a complementary and alternative therapy, acupuncture and moxibustion have shown dual clinical benefits in HCC: enhancing analgesia and reducing drug side effects while exerting antitumor effects through immune modulation, thereby improving patients' quality of life and treatment outcomes.

The development of liver cancer, from hepatitis and cirrhosis to hepatocellular carcinoma, is closely related to the spleen and liver in Traditional Chinese Medicine (TCM). Liver cancer is considered a disease of deficiency, primarily characterized by deficiency of the liver, spleen, and kidneys, while the manifestation involves stagnation of qi, damp-

heat, and stasis toxin.[37] Zusanli (ST36) is the He point of the Stomach Meridian of Foot-Yangming, as well as the Lower He point of the stomach fu-organ. It is a commonly used acupoint for disorders of the epigastrium and abdomen and is a key point for strengthening the body. The selection of Ganshu (BL18) is based on the therapeutic principle in TCM that states, "For diseases of a yin organ (zang), select the corresponding Back-Shu point located on the yang aspect of the body." Therefore, for liver diseases, Ganshu (BL18) on the back is selected for treatment.[38] Experimental studies have demonstrated that acupuncture at Zusanli (ST36) can inhibit the growth of tumor cells in H22 hepatoma-bearing mice.[21] Both moxibustion at Ganshu (BL18) and Zusanli (ST36) have been shown to effectively reduce cancer cell proliferation by modulating the Wnt signaling pathway.[39] Furthermore, direct moxibustion and ginger-partitioned moxibustion applied to Ganshu (BL18) alleviated DEN-induced inflammatory responses in rat hepatocytes, improved hepatocyte membrane permeability, and enhanced the self-repair capacity of liver cell.[38] The combination of Zusanli and Ganshu has the effects of soothing the liver and strengthening the spleen, reinforcing healthy qi to strengthen the body, regulating and harmonizing qi and blood, and resolving masses and eliminating accumulation, therefore, this study selected two points for intervention.

The spleen index serves as an important indicator of the body's immune status. In models of liver cancer, splenomegaly is often associated with portal hypertension and systemic immune dysregulation. Splenic dysfunction not only induces liver fibrosis but also alters hepatic immunoregulation, accelerating cirrhosis and suppressing liver regeneration capacity.[40] Studies indicated that splenectomy can help delay the progression of HCC, promote the recovery of liver function, and enhance anti-tumor immune responses.[41,42] Our results showing a reduced spleen index following treatment suggest that electroacupuncture and moxibustion may ameliorate splenic function and modulate systemic immune responses, which could be associated with their observed antitumor effects. Meanwhile, after moxibustion and electroacupuncture intervention in HCC mice, the degree of liver lobe adhesion, liver index were significantly reduced, the number of liver tumors, tumor load, the average diameter of tumors and volume of tumors were smaller compared to MG, which suggest that moxibustion and electroacupuncture can inhibit the growth of HCC tumors.

AFP, the most common serum test method in the monitoring and diagnosis of HCC has been challenged in its lower diagnostic sensitivity.[43] Therefore, AFP is generally used in combination with other serum biomarkers to detect AFP negative HCC, and AFP-L3 can improve the specificity of HCC diagnosis and is a new generation of diagnostic markers for HCC.[44] This study explored the efficacy of two intervention measures, moxibustion and electroacupuncture. Serological indicators showed that the protein contents of AFP and AFP-L3 in the model group were significantly higher than those in the normal group, while the two protein contents were significantly lower than those in the model group after moxibustion and electroacupuncture treatment. This shows that both moxibustion and electroacupuncture have improved liver function in HCC mice.

Study demonstrated that NSUN2 knockout could inhibit cellular process and tumor growth in HCC, which clarified NSUN2 has a regulatory effect on HCC cell proliferation and apoptosis.[45] This study investigated the effect of moxibustion and electroacupuncture on the expression of NSUN2 in HCC mice and was found that the protein and mRNA levels of NSUN2 in liver tissues were decreased significantly compared with MG after moxibustion and electroacupuncture. In summary, overexpression of NSUN2 promotes the proliferation and migration of HCC, but it can be blocked with moxibustion and electroacupuncture intervention, indicating that moxibustion and electroacupuncture intervention may affect the development of HCC by inhibiting the expression of NSUN2.

Cancer is composed of metabolically heterogeneous cells. To support maximal tumor growth, tumor and stromal cells, or metabolically diverse cancer cells, communicate by exchanging metabolites, including lactate—a phenomenon known as "metabolic coupling" or "metabolic symbiosis".[46,47] Glucose metabolism serves as the primary source of energy for life activities[48] and plays a critical role in cancer development. Even under oxygen-sufficient conditions, cancer cells preferentially utilize the glycolytic pathway and produce lactate, a phenomenon termed the "Warburg effect".[49,50] HK2 is the first rate-limiting enzyme involved in glucose metabolism after glucose enters the cell which catalyzes the conversion of glucose to G6P and is highly expressed in HCC tissues, directly correlating with pathological staging and patient prognosis.[51] And PFK1 is involved in the process of catalyzing G6P into F6P and subsequently converting F6P into fructose-1,6-bisphosphate.[52] PKM2 is a terminal enzyme in the glycolytic pathway that is upregulated in HCC and is associated with poor prognosis, and enhances the Warburg effect to promote HCC initiation and

metastasis by catalyzing the conversion of phosphoenolpyruvate (PEP) and ADP into pyruvate and ATP.[6,53] Studies have reported that HCC patients with higher PKM2 expression levels exhibit a higher recurrence rate compared to those with lower expression levels.[54] This study utilized targeted metabolomics analysis to examine differences in glycolytic metabolites between groups and identified significant variations in G6P, F6P, and PEP. The relative levels of G6P and F6P in the liver tissues were elevated in MG compared to NG, while moxibustion reduced the levels of G6P and F6P, and electroacupuncture reduced the level of G6P. These findings suggest that moxibustion and electroacupuncture may increase glucose uptake, leading to lower levels of G6P and F6P. Decreasing PEP levels, increasing PKM2 protein and mRNA expression, and elevating HK2 protein expression were explored in MG. In contrast, moxibustion and electroacupuncture intervention increased PEP levels, while reducing PKM2 protein and mRNA expression as well as HK2 protein expression. In summary, these results indicate that moxibustion and electroacupuncture may inhibit glycolytic terminal enzyme PKM2, thereby reducing PEP consumption, affecting lactate production, and ultimately suppressing the glycolytic process in HCC.

While both electroacupuncture and moxibustion are applied at identical acupoints, they exert their influence on HCC progression through different initial signaling mechanisms. Our study observed that both interventions converge on the suppression of the NSUN2-PKM2 glycolytic axis, suggesting that they may share a common downstream metabolic regulatory node in the context of HCC inhibition. However, a deeper analysis of the metabolic profiles altered by each intervention revealed that moxibustion exhibited a broader capacity for metabolic modulation, affecting a range of metabolites including G6P, F6P, PEP, GMP, and AMP. This indicates that moxibustion may induce a more comprehensive metabolic reprogramming and energy stress response. While, electroacupuncture did not show a pronounced effect on F6P and GMP regulation, suggesting that its influence on the metabolic network may be more focused yet remains sufficient to effectively inhibit the core pathway. Future studies are needed to further delineate the specific mechanistic differences between these two modalities.

This study has several limitations. The mechanistic conclusions rely primarily on correlative observations between moxibustion/electroacupuncture and reduced NSUN2/PKM2 levels, without direct functional validation (eg, rescuing NSUN2/PKM2 expression to reverse therapeutic effects). The absence of a sham acupuncture control complicates the interpretation of specific therapeutic effects versus non-specific physiological responses. Future studies should incorporate genetic or pharmacological interventions, rigorous control groups, and clinical research to strengthen the mechanistic and therapeutic implications of these findings.

Future directions for combination with current therapies. Although TACE and immune checkpoint inhibitors (ICIs) have become pivotal treatments for intermediate to advanced stage HCC, their clinical application is constrained by well documented limitations. Post TACE ischemia hypoxia can exacerbate immunosuppression within the tumor microenvironment and may trigger a “rebound invasion” growth pattern, while the efficacy of ICIs is often limited by treatment related adverse events in HCC. The mechanisms revealed in our study suggest that acupuncture may intervene in the metabolic reprogramming of residual tumor cells after TACE, providing a theoretical basis for suppressing invasive progression, and demonstrate its immunomodulatory potential (eg, regulating T cell subsets). Future research should focus on evaluating the effects of acupuncture combined with TACE on objective response rate, progression free survival, and quality of life, as well as examining the impact of acupuncture combined with immunotherapy on the tumor immune microenvironment, treatment response rate, and adverse event profiles. By advancing mechanism informed clinical studies, acupuncture and moxibustion hold promise as a valuable integrative component in the multidisciplinary management of HCC.

Conclusions

In conclusion, these findings elucidate that both electroacupuncture and moxibustion—despite their distinct biophysical nature—converge to inhibit the occurrence and progression of HCC by suppressing NSUN2-mediated glycolysis, with moxibustion potentially inducing a more extensive metabolic stress response. These findings not only provide a mechanistic basis for the observed clinical benefits of acupuncture in cancer patients, such as improved quality of life and symptom control, but also illuminate a translational bridge to potential combination therapy. While the correlative evidence presented strongly supports this mechanism, definitive establishment of causality would require

future functional validation through rescue experiments. Targeting the NSUN2-PKM2 metabolic-epigenetic node with acupuncture may offer a novel adjunctive strategy to enhance the efficacy or reduce the side effects of current standard HCC treatments, meriting further clinical investigation.

Data Sharing Statement

The datasets supporting the conclusions of this article can be provided by the corresponding author Luyi Wu.

Ethical Statement

The use of these animals was approved by the Animal Ethics Committee of Shanghai University of Traditional Chinese Medicine and was conducted strictly in accordance with the Management Specifications for Experimental Animals of Shanghai University of Traditional Chinese Medicine (Approval Number: PZSHUTCM210122012).

Acknowledgment

We gratefully acknowledge BioRender for providing the image materials used in this article (Agreement number: JV297TOQVQ).

Author Contributions

All authors made a significant contribution to the work reported, whether that is in the conception, study design, execution, acquisition of data, analysis and interpretation, or in all these areas; took part in drafting, revising or critically reviewing the article; gave final approval of the version to be published; have agreed on the journal to which the article has been submitted; and agree to be accountable for all aspects of the work.

Funding

This work was supported by Clinical Research Special Projects of Shanghai Municipal Health Commission (grant number 20244Y0065, 202440158), Shanghai "Science and Technology Innovation action Plan" Star Cultivation Sail Special Project (grant number 24YF2740600) and State Administration of Traditional Chinese Medicine high-level key discipline construction project (grant number zyyzdxk-2023068).

Disclosure

The authors report no conflicts of interest in this work.

References

1. Siegel RL, Giaquinto AN, Jemal A. Cancer statistics, 2024. *CA Cancer J Clin*. 2024;74(1):12–49. doi:10.3322/caac.21820
2. Zhou P, Zheng G, Li Y, Wu D, Chen Y. Construction of a circRNA-miRNA-mRNA network related to macrophage infiltration in hepatocellular carcinoma. *Front Genet*. 2020;11:1026. doi:10.3389/fgene.2020.01026
3. Dai W, Xu L, Yu X, et al. OGDHL silencing promotes hepatocellular carcinoma by reprogramming glutamine metabolism. *J Hepatol*. 2020;72(5):909–923. doi:10.1016/j.jhep.2019.12.015
4. Huang Q, Tan Y, Yin P, et al. Metabolic characterization of hepatocellular carcinoma using nontargeted tissue metabolomics. *Cancer Res*. 2013;73(16):4992–5002. doi:10.1158/0008-5472.CAN-13-0308
5. Karamafrooz A, Brennan J, Thomas DD, Parker LL. Integrated phosphoproteomics for identifying substrates of human protein kinase A (PRKACA) and its oncogenic mutant DNAJB1-PRKACA. *J Proteome Res*. 2021;20(10):4815–4830. doi:10.1021/acs.jproteome.1c00500
6. Feng J, Li J, Wu L, et al. Emerging roles and the regulation of aerobic glycolysis in hepatocellular carcinoma. *J Exp Clin Cancer Res CR*. 2020;39(1):126. doi:10.1186/s13046-020-01629-4
7. Martin SP, Fako V, Dang H, et al. PKM2 inhibition may reverse therapeutic resistance to transarterial chemoembolization in hepatocellular carcinoma. *J Exp Clin Cancer Res CR*. 2020;39(1):99. doi:10.1186/s13046-020-01605-y
8. Hu B, Yu M, Ma X, et al. IFNα potentiates anti-PD-1 efficacy by remodeling glucose metabolism in the hepatocellular carcinoma microenvironment. *Cancer Discov*. 2022;12(7):1718–1741. doi:10.1158/2159-8290.CD-21-1022
9. Yu Q, Dai W, Ji J, et al. Sodium butyrate inhibits aerobic glycolysis of hepatocellular carcinoma cells via the c-myc/hexokinase 2 pathway. *J Cell Mol Med*. 2022;26(10):3031–3045. doi:10.1111/jcmm.17322
10. Feng J, Wu L, Ji J, et al. PKM2 is the target of proanthocyanidin B2 during the inhibition of hepatocellular carcinoma. *J Exp Clin Cancer Res CR*. 2019;38(1):204. doi:10.1186/s13046-019-1194-z
11. Chellamuthu A, Gray SG. The RNA methyltransferase NSUN2 and its potential roles in cancer. *Cells*. 2020;9(8):1758. doi:10.3390/cells9081758

12. Hussain S, Benavente SB, Nascimento E, et al. The nucleolar RNA methyltransferase Misu (NSun2) is required for mitotic spindle stability. *J Cell Biol*. 2009;186(1):27–40. doi:10.1083/jcb.200810180
13. Khan MA, Rafiq MA, Noor A, et al. Mutation in NSUN2, which encodes an RNA methyltransferase, causes autosomal-recessive intellectual disability. *Am J Hum Genet*. 2012;90(5):856–863. doi:10.1016/j.ajhg.2012.03.023
14. Xing J, Yi J, Cai X, et al. NSun2 promotes cell growth via elevating cyclin-dependent kinase 1 translation. *Mol Cell Biol*. 2015;35(23):4043–4052. doi:10.1128/MCB.00742-15
15. Qi Q, Zhong R, Huang Y, et al. The RNA M5C methyltransferase NSUN2 promotes progression of hepatocellular carcinoma by enhancing PKM2-mediated glycolysis. *Cell Death Dis*. 2025;16(1):1–12. doi:10.1038/s41419-025-07414-5
16. Zhang Y, Shen Y, Zhu L, et al. Effect of acupuncture and moxibustion on immunoregulation mediated by DNA hydroxymethylases TETs in rats with ulcerative colitis. *Shanghai J Acupunct Moxibustion*. 2025;44(6):750–759. doi:10.13460/j.issn.1005-0957.2024.13.3038
17. Xu HX, Zhu L, Wu LY, et al. Effects of acupuncture and moxibustion on DNA methylation profiles in colonic tissue of Crohn disease rats. *China J Tradit Chin Med Pharm*. 2025;40(5):2117–2122.
18. Qi Q, Wang XM, Wu HG, et al. Effects of acupuncture and moxibustion on colonic DNA methyltransferase under hpoxic environment in rats with Crohn's disease. *World Chin Med*. 2022;17(3):317–322.
19. Shen JM, Zhang WT, Wu QY, Wang D. Clinical study of electroacupuncture for cancer pain of hepatoma. *J Liaoning Univ Tradit Chin Med*. 2013;15(9):189–191. doi:10.13194/j.issn.1673-842x.2013.09.023
20. Chen ML. Observation on the Clinical Curative Effect of Electroacupuncture at Siguan Acupoints Combined with Ear Acupoint Pressing Beans on Liver Cancer Pain. *Chongqing Medical University*; 2022. doi:10.27674/d.cnki.gcyku.2021.001320
21. Zhang YE. Effects of Acupuncture on Immune Function Andapoptosis-Related Proteins in Mouse with Transplanting Iiver Cancer. *Guangzhou University of Chinese Medicine*; 2008. Available from: https://kns.cnki.net/kcms2/article/abstract?v=Ap1IM-J3Ck2o374TNjNEnK95zP7KNfkJm4enYzUC00Djh4r7agbsct_k-X2rEbYY2qoohu8hhRfgKzLf4WU-Gi9kV2SQPh0twiHi8aaPjO1rANq6wHG0vFTwcMarYNdSW1jCV8s-ditXyh8BVquPBXExWGD0whrGaibqkLTDdFI0oAA7tM-bvHINucLeRMuZ&uniplatform=NZKPT&language=CHS
22. Fang J, Wu YQ, Huang XY, Wang R. Study on retarding growth trend effect of electroacupuncture in hepG2 hepatocellular carcinoma in nude mice based on microRNA. *Chin J Tradit Med Sci Technol*. 2023;30(1):8–13.
23. Chen D, Chi M, Yan YT. Clinical observation of moxibustion at Guanyuan and Qihai points in patients with advanced liver cancer. *Chin J Integr Tradit West Med Liver Dis*. 2019;29(1):35–37.
24. Dhar D, Baglieri J, Kisseleva T, Brenner DA. Mechanisms of liver fibrosis and its role in liver cancer. *Exp Biol Med*. 2020;245(2):96–108. doi:10.1177/1535370219898141
25. Kocabayoglu P, Lade A, Lee YA, et al. β-PDGF receptor expressed by hepatic stellate cells regulates fibrosis in murine liver injury, but not carcinogenesis. *J Hepatol*. 2015;63(1):141–147. doi:10.1016/j.jhep.2015.01.036
26. Chen T, Sun D, Wang Q, et al. α-Hederin inhibits the proliferation of hepatocellular carcinoma cells via hippo-yes-associated protein signaling pathway. *Front Oncol*. 2022;12:839603. doi:10.3389/fonc.2022.839603
27. Fausto N, Campbell JS. Mouse models of hepatocellular carcinoma. *Semin Liver Dis*. 2010;30(1):87–98. doi:10.1055/s-0030-1247135
28. Kulik L, El-Serag HB. Epidemiology and management of hepatocellular carcinoma. *Gastroenterology*. 2019;156(2):477–491.e1. doi:10.1053/j.gastro.2018.08.065
29. Zhou J, Sun H, Wang Z, et al. Guidelines for the diagnosis and treatment of hepatocellular carcinoma (2019 edition). *Liver Cancer*. 2020;9(6):682–720. doi:10.1159/000509424
30. Zhu L, Li J, Wang ZQ, et al. Treatment of moderate-to-severe pain in hepatocellular carcinoma with transcutaneous electrical acupoint stimulation: a randomized controlled trial. *J Pain Res*. 2024;17:1583–1594. doi:10.2147/JPR.S456874
31. Huang XB, Qiu DS, Qiu Q, Wu XL, Xie DY, Chen RX. Heat-sensitive moxibustion combined with immune-targeted therapy for 2 cases of giant liver cancer. *Jiangxi J Tradit Chin Med*. 2022;53(8):51–55+58.
32. Liu ZY, Zhang HB, Luo Y, et al. Curative effect of YU Yun pulse-feeling-based acupuncture therapy for treatment of middle-late liver cancer. *J Guangzhou Univ Tradit Chin Med*. 2018;35(1):66–69. doi:10.13359/j.cnki.gzxbtcm.2018.01.0014
33. Huang JC, Zhao PC, Li R, Xu L, Shi XW, Zhang M. Clinical observation on the treatment of 36 cases of primary liver cancer with fire needle surrounding acupuncture combined with syndrome differentiation. *Chin J Clin*. 2016;44(12):91–93.
34. Lai M, Wang SM, Zhang WL, et al. Effects of electroacupuncture on tumor growth and immune function in the Walker-256 model rat. *Chin Acupunct Moxibustion*. 2008;28(8):607–609.
35. Wang R. Research on Felicitous Repression of Cancer by Electro-Acupuncture Enhances Inhibition of Mir-409-5p on TGF-B1 Signal Pathway. *Chengdu University of Traditional Chinese Medicine*; 2017.
36. Yang L, Zhou Y, Huang Z, et al. Electroacupuncture promotes liver regeneration by activating DMV acetylcholinergic neurons-vagus-macrophage axis in 70% partial hepatectomy of mice. *Adv Sci Weinh Baden-Wurtt Ger*. 2024;11(32):e2402856. doi:10.1002/advs.202402856
37. Wang WQ, Gao ZH, Yin CJ. A methodological study of traditional Chinese medicine treatment of primary liver cancer. *J Clin Hepatol*. 2021;37(9):2009–2015.
38. Jia WR, Dong F, Xie XL, et al. Effects of moxibustion at "Ganshu" (BL18) on serum alpha-fatoprotein and liver livin levels in rats with precancerous lesion of primary hepatocellular carcinoma. *Acupunct Res*. 2014;39(3):211–215. doi:10.13702/j.1000-0607.2014.03.009
39. Wang Y, Guan ST, Zhang XL, et al. Relative genetic expression influence on primary hepatic carcinoma rats' wnt signal channel by scared moxibustion pre-process. *Chin Arch Tradit Chin Med*. 2017;35(5):1225–1228. doi:10.13193/j.issn.1673-7717.2017.05.047
40. Jessica C, Chen XX, Chen YJ. Role of the spleen in patients with liver cancer and cirrhosis. *J Surg Concepts Pract*. 2023;28(4):394–398. doi:10.16139/j.1007-9610.2023.04.018
41. Elchaninov AV, Fatkhudinov TK, Vishnyakova PA, et al. Molecular mechanisms of splenectomy-induced hepatocyte proliferation. *PLoS One*. 2020;15(6):e0233767. doi:10.1371/journal.pone.0233767
42. Zhu WG. Effects of combined hepatectomy and splenectomy on liver function and immune parameters in patients with hepatocellular carcinoma complicated by liver cirrhosis and hypersplenism. *Chin J Lab Diagn*. 2015;19(1):108–110.
43. Fu L, Yao T, Chen Q, Mo X, Hu Y, Guo J. Screening differential circular RNA expression profiles reveals hsa_circ_0004018 is associated with hepatocellular carcinoma. *Oncotarget*. 2017;8(35):58405–58416. doi:10.18632/oncotarget.16881

44. Park SJ, Jang JY, Jeong SW, et al. Usefulness of AFP, AFP-L3, and PIVKA-II, and their combinations in diagnosing hepatocellular carcinoma. *Medicine*. 2017;96(11):e5811. doi:10.1097/MD.0000000000005811
45. Zhai CT, Tian YC, Tang ZX, Shao LJ. RNA methyltransferase NSUN2 promotes growth of hepatocellular carcinoma cells by regulating fizzy-related-1 in vitro and in vivo. *Kaohsiung J Med Sci*. 2021;37(11):991–999. doi:10.1002/kjm2.12430
46. Avagliano A, Granato G, Ruocco MR, et al. Metabolic reprogramming of cancer associated fibroblasts: the slavery of stromal fibroblasts. *BioMed Res Int*. 2018;2018:6075403. doi:10.1155/2018/6075403
47. Yoshida GJ. Metabolic reprogramming: the emerging concept and associated therapeutic strategies. *J Exp Clin Cancer Res CR*. 2015;34:111. doi:10.1186/s13046-015-0221-y
48. Gui X, Zhang H, Zhang R, et al. Exosomes incorporated with black phosphorus quantum dots attenuate retinal angiogenesis via disrupting glucose metabolism. *Mater Today Bio*. 2023;19:100602. doi:10.1016/j.mtbio.2023.100602
49. Potter M, Newport E, Morten KJ. The Warburg effect: 80 years on. *Biochem Soc Trans*. 2016;44(5):1499–1505. doi:10.1042/BST20160094
50. Liberti MV, Locasale JW. The Warburg effect: how does it benefit cancer cells? *Trends Biochem Sci*. 2016;41(3):211–218. doi:10.1016/j.tibs.2015.12.001
51. Lis P, Dyląg M, Niedźwiecka K, et al. The HK2 dependent "Warburg Effect" and mitochondrial oxidative phosphorylation in cancer: targets for effective therapy with 3-bromopyruvate. *Molecules*. 2016;21(12):1730. doi:10.3390/molecules21121730
52. Kanai S, Shimada T, Narita T, Okabayashi K. Phosphofructokinase-1 subunit composition and activity in the skeletal muscle, liver, and brain of dogs. *J Vet Med Sci*. 2019;81(5):712–716. doi:10.1292/jvms.19-0049
53. Li TE, Wang S, Shen XT, et al. PKM2 drives hepatocellular carcinoma progression by inducing immunosuppressive microenvironment. *Front Immunol*. 2020;11:589997. doi:10.3389/fimmu.2020.589997
54. Li YH, Li XF, Liu JT, et al. PKM2, a potential target for regulating cancer. *Gene*. 2018;668:48–53. doi:10.1016/j.gene.2018.05.038